ARTICLES

Influence of Disorder on Electronic Excited States: An Experimental and Numerical Study of Alkylthiotriphenylene Columnar Phases

Sylvie Marguet,[†] Dimitra Markovitsi,*[,†] Philippe Millié,[‡] and Hervé Sigal[†]

CEA/Saclay, DRECAM, 91191 Gif-sur-Yvette, France

Sandeep Kumar

Centre for Liquid Crystal Research, P.O. Box 1329, Jalahalli, Bangalore, 560013, India

Received: January 5, 1998; In Final Form: March 16, 1998

The spectroscopic properties of discotic hexa-alkylthiotriphenylenes are studied in solution and thin films and compared to those of hexa-alkyloxytriphenylenes. The solution properties are analyzed in the light of CS-INDO-CIPSI quantum chemistry calculations. The absorption maximum is assigned to the degenerate $S_0 \rightarrow S_4$ transition. The fluorescence of the neat phases is attributed to weakly bound excimers. The phase transition leading from ordered to disordered columnar stacks induces an increase in the oscillator strength of the $S_0 \rightarrow S_1$ transition and favors excimer formation. The influence of structural disorder on the properties of the delocalized states is rationalized by using various approximations within the frame of the exciton theory; three models for the calculation of the exciton coupling (point dipole, extended dipole, atomic transition charge distribution) are tested, short and long range interactions are considered, and the introduction of a dielectric constant is discussed. The best agreement between experimental and calculated absorption maxima is obtained using the atomic charge transition model. Off-diagonal disorder is correlated to structural disorder by changing the orientation and the position of the molecules within the aggregate. The case of degenerate molecular states is compared to that of nondegenerate ones. Orientational disorder has a dramatic effect on the energy and the localization of the upper eigenstate when molecular states are nondegenerate. Conversely, the properties of degenerate eigenstates are quite insensitive to orientational disorder. The magnitude of the off-diagonal disorder induced by positional disorder largely depends on the model used in the calculation of the exciton coupling. The results of the numerical calculations are in agreement with the small change observed in the neat phases absorption maxima upon a quasi one-dimensional melting of columnar stacks.

1. Introduction

The influence of disorder on the electronic excited states of molecular assemblies as well as on charge and energy transport in these systems is the subject of numerous studies. This research topic is important for molecular electronics because structural disorder is an intrinsic characteristic of molecular materials. The extent to which disorder in the molecular arrangement will influence a given macroscopic property is related to the electronic properties of molecules. Therefore, it is important to be able to predict molecular properties required to make the material behavior less sensitive to disorder. This prediction depends on the level of approximation of the theoretical models used to correlate the macrosopic properties to the molecular ones. For example, an investigation of the excitation hopping in columnar liquid crystals, showing that the hopping times derived from experimental data, highly depend on the model used for their analysis.[1]

Most studies dealing with the influence of disorder on electronic excited states are carried out within the frame of the exciton theory, describing the excited states of the examined systems as linear combinations of the excited states localized on each molecule.[2,3] The disorder in the molecular arrangement is depicted by a disorder in the diagonal or off-diagonal terms in the Hamiltonian matrix,[4−8] respectively representing the excitation energy of the states localized on each chromophore and the coupling between transition moments. In these studies, the molecules are considered as points. Knowing that the point dipole model is a poor approximation when the interchromophore separation is small compared to their planar dimensions,[9,10] one can ask if the quantitative conclusions of the above-mentioned studies remain valid when the level of approximation for the exciton coupling is improved.

A model based on the exciton theory and on semiempirical quantum chemistry methods[11] allowing the representation of molecules no longer as points but atom-by-atom was proposed a few years ago. The diagonal and off-diagonal terms in the Hamiltonian matrix can be calculated by taking into account both the electronic structure of the molecules and their coordinates within the aggregate. This methodology was applied to calculate the eigenstate properties of columnar aggregates

[†] SCM (Division of CEA/Saclay) CNRS-URA 331.
[‡] SPAM (Division of CEA/Saclay).

S1089-5647(98)00623-3 CCC: $15.00
Published on Web 05/23/1998

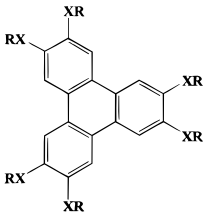

Figure 1. The studied hexa-alkylthiotriphenylenes (HnTT: X = S, R = C_nH_{2n+1}) and hexaalkyloxytriphenylenes (HnOT: X = O, R = C_nH_{2n+1}).

formed by triarylpyrylium salts[11] and hexa-alkyloxytriphenylenes.[1] More recently, similar calculations were carried out for conjugated oligomers.[12]

The question arises whether it is possible to obtain a quantitative description of the influence of disorder on the excited states of molecular assemblies. For this purpose, the calculated properties must be compared with observables obtained for a physical system whose degree of order can be experimentally controlled. The hexa-hexylthiotriphenylene (H6TT) shown in Figure 1 is particularly attractive from this point of view, because it presents a rich polymorphism.[13−17] At room temperature it forms a K crystalline phase having a monoclinic structure. Upon heating to 62 °C, a solid columnar phase H appears which is transformed to a columnar liquid crystal (D_h) at 70 °C. The latter is stable up to 93 °C, temperature at which an isotropic liquid (I) is obtained.

$$K \xleftrightarrow{62\ ^\circ C} H \xleftrightarrow{70\ ^\circ C} D_h \xleftrightarrow{93\ ^\circ C} I$$

The H → D_h transition is a unique example of quasi-one-dimensional melting of molecular stacks. In both the H and D_h phases, the column axes form a hexagonal lattice. Within the columns of the H phase, adjacent molecules are rotated by 45° giving rise to a helical stucture. Upon the H → D_h transition, the intercolumnar distance and the average stacking distance remain practically the same, while the helical structure is destroyed, (i.e., the molecular orientation around the column axis becomes random). Furthermore, the amplitude of the molecular motion around the average position of the aromatic cores in the stacks increases and the correlation between columns is lost.

We have undertaken an investigation of H6TT in solution[18] and its various organized phases. Our aim was 2-fold. On one hand, we wanted to characterize the excited states associated to photon absorption and emission. To that end, we used, jointly to the experiments, quantum chemistry calculations based on the CS-INDO-CIPSI (Conformation spectra−intermediate neglect of differential overlap−configuration interaction by perturbative selected iterations) method. We also wanted to see how changes in the molecular arrangement induced by phase transitions affect some basic photophysical properties. On the other hand, we intended to rationalize the influence of the structural disorder on the properties of the exciton states. In particular, we focused on the off-diagonal disorder induced by rotational and positional structural disorder. For this purpose, it was important to compare the experimental results to the results of numerical calculations obtained by various approximations of the exciton model. These approximations refer to the calculation of the exciton coupling (point dipole, extended dipole, atomic transition charge distribution), the consideration of short or long range interactions and the use of a dielectric constant. The strong electronic transition of triphenylenes being degenerate, it seemed important to compare the behavior of eigenstates built on degenerate molecular states to that of eigenstates built on nondegenerate ones, commonly studied in the literature.

The experimental properties obtained for the sulfur derivative H6TT are compared to those found for the oxygen derivative H5OT (Figure 1). This enables us to make a connection with previous photophysical studies of hexa-alkyloxytriphenylenes.[1]

The paper is organized as follows. The experimental details are given in section 2. In section 3, the procedure followed both in the quantum chemistry calculations (section 3.1) and in the calculation of the exciton matrix are described (section 3.2). Section 4 deals with "isolated" chromophores. The properties of the electronic excited states obtained by quantum chemistry calculations and the photophysical properties of solutions are discussed. The photophysical properties of the organized phases are described in section 5, and the exciton states are studied numerically in section 6. In section 7, a quantitative comparison of the experimental and calculated exciton shift values is made. Finally, in section 8, the main results are summarized and conclusions are drawn.

2. Experimental Details

2.1. Synthesis of the Compounds. 2,3,6,7,10,11-hexa-*n*-hexylthiotriphenylene was prepared following a modification of previously reported methods.[16,20] Potassium-*t*-butoxide (4.17 g, 34 mmol) was added to a solution of hexanethiol (4.04 g, 34 mmol) in 1-methyl-2-pyrrolidinone (25 mL). After the solution was heated at 100 °C for 5 min and then cooled to 70 °C, hexabromotriphenylene (2.0 g, 2.85 mmol) was added. The reaction mixture was stirred at 70 °C, and 1-bromohexane was added (2.8 g, 17 mmol). It was left to react overnight. After addition of water, the compound was extracted using diethyl ether. The crude product was purified by column chromatography over silica gel eluting with 2.5% ethyl acetate in *n*-hexane. The powder compound was dissolved in diethyl ether and passed through 0.2 mm filter paper. Finally, it was recrystallized in an ethyl ether/acetone mixture. Yield was 83%.

2,3,6,7,10,11-Hexa-*n*-pentyloxytriphenylene was prepared following a modification of the method described in ref 21. Anhydrous ferric chloride (4.8, 0.03 mol) was added to a solution of 1,2-dipentyloxy benzene (2.5 g, 0.01 mol) in 15 mL of dry dichloromethane containing 1% concentrated H_2SO_4. The reaction mixture was stirred at room temperature for 20 min under anhydrous conditions and was poured over cold methanol (50 mL). The white precipitate was filtered out, washed with methanol, and purified over neutral alumina eluting with 2% ethyl acetate in *n*-hexane. The powder compound was dissolved in diethyl ether and passed through 0.2 mm filter paper. Finally, it was recrystallized in an ethyl ether/methanol mixture. Yield was 50%.

Remark: Filtration improved the purity of the compound by eliminating alumina particles. Thus, the maximum molar extinction coefficient found in this work ($1.2 \times 10^5\ M^{-1}\ cm^{-1}$, Figure 2) is more accurate than that reported in ref 1 ($10^5\ M^{-1}cm^{-1}$).

2.2. Apparatus and Experimental Procedure. In order to record absorption spectra of thin film in the region of the absorption maximum without saturation of the detector, it was necessary to use spectroscopic cells whose thickness was smaller than 0.2 μm. These cells were prepared by pressing together two quartz slides and filled by capillary effect upon heating the powder compound to its isotropic phase. The planeity of these quartz slides was better than 0.1 μm. An appropriate cleaning procedure of the quartz slides was required; they were

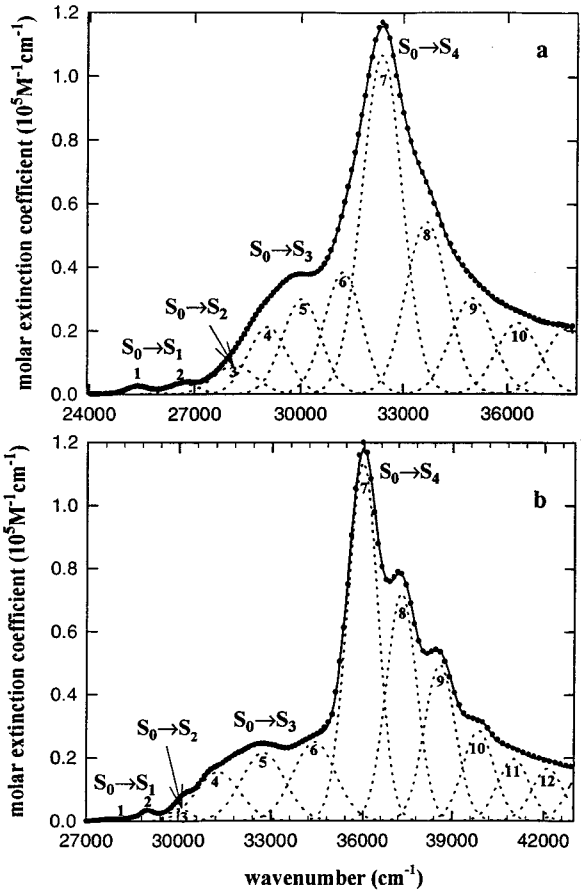

Figure 2. Decomposition of the absorption spectra of (a) H6TT and (b) H5OT in *n*-heptane into Gaussian bands according to a vibronic progression model. Attribution of these Gaussians to the electronic transitions: bands 1,2 ($S_0 \rightarrow S_1$), band 3 ($S_0 \rightarrow S_2$), bands 4−6 ($S_0 \rightarrow S_3$), bands 6−10 ($S_0 \rightarrow S_4$).

sonicated successively in dichloromethane, detergent solution, distilled water and ethanol (20 min each time), and then pyrolyzed at 300 °C. The determination of the molar absorption coefficient corresponding to the $S_0 \rightarrow S_1$ transition for the various phases (K, H, D_h) was achieved by means of calibrated Shinshikyu silica spacers (Dodwell marketing services, Japan) of various sizes 1.3, 5, or 10 μm. We verified that the absorption spectra obtained for different cell thicknesses overlap after normalization by taking the optical path-length into account. The sample alignment was checked by using a LEITZ polarizing microscope equipped with a METTLER temperature controller. For spectroscopic measurements, the temperature of thin films was regulated using either an Oxford Instruments liquid nitrogen cryostat (DN1704) equipped with a PID temperature controller unit (ITC-4) or a LINKAM heating stage (LTS 350) equipped with a LINKAM TP 92 temperature controller. A waiting time of 30 min was necessary to reach thermal equilibrium with the cryostat, whereas a few minutes were sufficient with the heating stage.

Steady-state absorption spectra were recorded with a PERKIN ELMER spectrophotometer (Lambda 900). Steady-state fluorescence emission and excitation spectra were recorded with a SPEX Fluorolog-2 spectrofluorometer; the spectra were corrected for the spectral response of the dispersing elements and the photomultiplier. For the neat phases, the exciting beam was perpendicular to the surface of the cell and fluorescence was collected at an angle of 20° with respect to the incident beam. Fluorescence quantum yields were determined using dihydrate quinine sulfate in 0.1 mol dm^{-3} $HClO_4$ as a reference (Φ_f = 0.59).[22] Fluorescence decays were obtained by the single photon counting technique. The excitation source was the second harmonic (λ_{ex} = 300 nm) of a dye laser synchronously pumped by a mode-locked Nd:Yag laser. A Glan−Thomson prism, forming an angle of 54.7° with the polarization direction of the exciting beam, was positioned in front of the monochromator. The detector was a microchannel plate (R1564 U Hamamatsu) providing an instrumental response function of 60 ps (fwhm).

3. Methods of Calculation

3.1. CS-INDO-CIPSI Calculations. The calculation of excited electronic states of large aromatic compounds, using semiempirical methods of quantum chemistry, is confronted with several obstacles that are the large number of bielectronic integrals and the size of the configuration interaction (CI) matrix. In general, reliable methods have to take into account both, the correlation energy and the reorganization of the whole σ system in the excited states. A new CS-INDO-CIPSI-type method allowing the resolution of these difficulties was recently developped by Germain and Millié.[23] This new method, in which the π and σ system are distinct and the σ molecular orbitals (MO) localized, has proved successful in studying the electronic states of small-sized, medium-sized,[23,24] and even very large chromophores.[25]

Since the length of the lateral alkyl chains does not have significant effects on the excited-state properties,[1] we performed our calculations for H1OT and H1TT bearing six methyloxy and six methylthio groups, respectively (Figure 1). Geometry optimization of the two compounds H1OT and H1TT was performed with the MOPAC package[26] using AM1 force field. Both ground-state geometries obtained from this optimization have a D_{3h} symmetry and greatly resemble that of the conformer "a" of ref 1. The two X−CH_3 bonds of each phenyl ring are in the plane of the aromatic core and point to opposite directions.

The calculation of the electronic states of H1OT and H1TT were performed by the previously cited CS-INDO-CIPSI method in the whole MO basis set (78 occupied orbitals and 66 virtual orbitals). No d orbitals were considered in the case of sulfur derivative H1TT because the sulfur atoms are divalent. Within this method, a preliminary singly-CI calculation is required before the CIPSI calculations in order to determine the natural orbitals.[23,25] From such a preliminary S-CI treatment, the six highest occupied MOs and the six lowest virtual MOs (all in the π system) were found to be involved in the initial variational S subspace of CIPSI. In the localization procedure of the σ system, the topological criterion called "2" in ref 23 was used. This approximation allowed us to reduce the number of two-electron integrals from 54.5×10^6 to 1.6×10^6. CIPSI calculations were performed using the two-classes version of the CIPSI algorithm.[27,28] A Moller−Plesset partition was used in the perturbation treatment and the threshold η, used in the iterative construction of the S variational space, was equal to 0.07. Following the CIPSI procedure, a final CI calculation was performed in order to obtain the dipole moments and the transition dipole moments. This was done by including in the CI matrix all determinants having a coefficient larger than 0.01 in the CIPSI procedure.

3.2. Exciton Theory Calculations. *3.2.1 General Considerations.* The Frenkel exciton model, widely used to analyze the excited states of molecular assemblies, does not consider intermolecular charge transfer states. Indeed, within this model, the excited states of the super system are described as a linear combination of the excited states localized on each chromophore:[2,3]

$$|k\rangle = \sum_{n=1}^{N} \sum_{i=1}^{I} C_{k,n}^{i} |\Psi_n^i\rangle \quad (1)$$

N denotes the number of chromophores of the aggregate and *I* the number of singlet electronic states that has to be considered on each chromophore. Ψ_n^i is the wave function of the super system when the molecule *n* is in its *i*th singlet excited state (ϕ_n^i wave function) whereas all the other molecules *m* are in their ground state (ϕ_m^0 wave functions):

$$\Psi_n^i = \phi_n^i \prod_{m \neq n} \phi_m^0 \quad (2)$$

Inherent to the exciton model is the assumption that the coupling between two configurations localized on two different molecules (e.g., $\pi_m \rightarrow \pi^*_m$ and $\pi_n \rightarrow \pi^*_n$) is much smaller than the coupling between two configurations localized on the same molecule (e.g., $\pi^1_m \rightarrow \pi^{2*}_m$ and $\pi^3_m \rightarrow \pi^{4*}_m$). In other words, intermolecular interactions are assumed to be weak with respect to intramolecular interactions in such a way that it is possible to decompose the total Hamiltonian (*H*) of the super system as the sum of the *N* Hamiltonians of the isolated molecules (H_0) plus an interaction operator *V*:

$$H = \sum_{n=1}^{N} + V = H_0 + V \quad (3)$$

In the NDO-type (neglect of differential overlap) semiempirical methods, the Ψ_n^i wave functions are orthogonal because of the orthogonality of the molecular orbitals (MO) which are totally localized on a single chromophore. The orbital overlap between any MO of the chromophore *m* and any MO of the chromophore *n*, ($n \neq m$) is equal to zero and hence the intermolecular interactions arising from orbital penetration are neglected. Ab initio calculations, have shown that these interactions can become significant at short distance, especially in the case of weak transitions.[29,30]

The Ψ_n^i eigenfunctions of H_0 form the basis of the total Hamiltonian matrix, the so-called exciton matrix. A full diagonalization of the exciton matrix provides the eigenvectors ($C_{k,n}^i$) and the eigenvalues (E_k) corresponding to the *NI* eigenstates $|k\rangle$ of the super system.

The diagonal term $\langle\Psi_n^i|H|\Psi_n^i\rangle$ of the exciton matrix represents the $S_0 \rightarrow S_i$ excitation energy of the molecule *n* "solvated" within the aggregate in the manner of solvent molecules. This diagonal terms can be calculated combining quantum chemistry calculations and molecular interaction calculations based, for example, on the semiempirical Claverie's method.[31] Intermolecular interactions are rationalized as the sum of electrostatic, polarization, dispersion, and repulsion terms. In the case of ionic compounds and for compounds whose transition induces an important variation in the atomic charge distribution, the electrostatic term is predominant, and thus, the solvation energy can be calculated with a good accuracy.[11] Conversely, for the triphenylene derivatives examined here, both the net atomic charges and the photoinduced variation of the atomic charges are very weak.[1] In this case, the predominant term in the interaction energy is no more the electrostatic but the dispersion term which cannot be calculated with acceptable accuracy for the excited states. Therefore, the solvation energy cannot be correctly calculated for such chromophores. The electrostatic energies involved in the calculation of the diagonal term *n* are of two kinds, either $E_{n,m\neq n}^{i,0}$ or $E_{n,m\neq n}^{0,0}$, where $E_{n,m\neq n}^{i,0}$ denotes the interaction energy between the molecule *n* in its *i*th excited state (S_i) and the molecule *m* in its ground state (S_0), and $E_{n,m\neq n}^{0,0}$ denotes the interaction energy when both molecules are in their ground state. The calculation of these electrostatic interactions requires a representation of the electronic densities of the S_0 and S_i states.

The off-diagonal terms $\langle\Psi_n^i|H|\Psi_n^i\rangle$ of the exciton matrix can be written as $V_{n,m}^{i,j} = \langle\phi_n^i\,\phi_m^0|V|\phi_n^0\,\phi_m^j\rangle$ where $V_{n,m}^{i,j}$ is the so-called exciton coupling. The approximation that the intermolecular electron exchange terms are negligible, the exciton coupling $V_{n,m}^{i,j}$ represents the electrostatic interaction between the two transition electronic densities, corresponding to $S_0 \rightarrow S_i$ and $S_0 \rightarrow S_j$. Here again, a representation of the transition electronic density based on a multipolar multicenter development is required in order to obtain accurate results. We have shown[1] that this development can be limited to one charge and one elementary dipole on each atom of the molecule. When the electronic transition is mainly described by $\pi \rightarrow \pi^*$ configurations, this development can be restricted to one charge on each atom. Indeed, in the INDO approximation, the elementary atomic dipoles arise from the monocentric $\langle s|r|p\rangle$ integrals between a s-type AO and a p-type AO. These monocentric monoelectronic integrals are only involved when the σ system is involved (i.e., when the electronic transition is described with $\sigma \rightarrow \pi^*$ (e.g., $n \rightarrow \pi^*$), $\pi \rightarrow \sigma^*$ or $\sigma \rightarrow \sigma^*$ configurations). This representation of the transition electronic density as a *multicentric monopole* expansion is called in the following, the *atomic transition charge distribution*.

It is worth-stressing that the usefulness of the exciton model is restricted to the case where the exciton coupling is larger than the static and dynamic fluctuations of the diagonal terms including the Boltzmann factor (*kT*). Indeed, when the total exciton coupling (coulomb + exchange + orbital penetration) is much smaller than variations of the diagonal terms, the eigenstates are localized and the eigenvalues correspond to the excitation energies of noninteracting chromophores. For this reason, within the formalism used in this study, the exciton model is of no use for the symmetry-forbidden $S_0 \rightarrow S_1$ transition of H1TT and H10T.

3.2.2. Approximations in the Calculation of the Exciton Matrix. In this section, we comment on four approximations which are often made in the exciton model. The first is related to the number of the electronic states of the molecule that has to be taken into consideration. The second is related to the diagonal terms of the exciton matrix, the third concerns the structure of the matrix and the fourth is related to the calculation of the exciton coupling.

(i) The study of the exciton states arising from an electronic S_i state has to involve all the S_j electronic states which are "close" to S_i. This means all the S_j states whose exciton band may interfere with the exciton band of the S_i state. Therefore, the two important parameters are the energy difference between the S_i and S_j states and the intensities of the transition dipole moments $S_0 \rightarrow S_i$ and $S_0 \rightarrow S_j$. In the numerical calculations presented in section 6 the exciton states are built on the degenerate S_4 state of H1TT. In this particular case, it is reasonable to neglect both the S_3 and S_5 states. Since only one transition is considered in the exciton matrix, $V_{n,m}^{i,j}$ is simplified to $V_{n,m}$ in the following. Since the transition is degenerate, there are four coupling terms between two distinct chromophores *m* and *n*. The off-diagonal term localized on the chromophore *n* ($V_{n,n}^{I,II}$ where I and II represent the two components of the degenerate transition) is taken equal to zero because this term is equal to zero for the isolated chromophore.

(ii) A current approximation is the assumption that all diagonal terms are equal. This approximation is very reasonable when the molecular transitions do not present any intramolecular charge transfer character or when the permanent dipole moments are zero for symmetry reasons. As an illustration of the accuracy of this approximation, it is worth remembering that, for a columnar aggregate of H1OT, the differences between the excitation energies of the molecules within the aggregate due to intermolecular electrostatic interactions, were found to be smaller than 70 cm^{-1} for $S_0 \rightarrow S_1$ and equal to about 130 cm^{-1} for $S_0 \rightarrow S_4$.[1] These energy differences are mainly observed at the two ends of the aggregate whereas the excitation energies are roughly constant within the aggregate. This is the so-called edge effect. On the other hand, large variations of the diagonal terms are expected in the case of ionic compounds or in the case of the intramolecular charge transfer states.[11]

(iii) In the nearest neighbor approximation, only the short-range interactions (i.e., only $V_{n,n\pm1}$ terms) are taken into consideration, whereas all the other off-diagonal terms are taken equal to zero. When all diagonal terms are equal, the structure of the excitonic matrix is that of a Hückel matrix for a polyene chain and whatever the values of these off-diagonal terms $V_{n,n\pm1}$, the eigenstate energies are always symmetrically distributed around the energy of the isolated chromophores. This distribution of the energies of the eigenstates around the energy of the isolated chromophore is used as a parameter allowing us to estimate the error made when the long-range interactions are neglected (section 6).

(iv) The fourth approximation is related to the model used in the calculation of the exciton coupling. Three models are presented below by increasing order of accuracy.

(a) In the *point dipole* model, the exciton coupling is simplified to the interaction between two transition dipole moments. This model is still widely used in the literature, although it was pointed out already in 1964 that it is not valid when the separation of the chromophores is small compared to their planar dimensions.[9] In the case of the columnar aggregates, the calculation of the exciton coupling in the point dipole approximation is given by

$$V_{n,m} = \frac{\mu\mu \cos\theta_{n,m}}{R^3} \tag{4}$$

where $\theta_{n,m}$ denotes the rotation angle between the two molecules n and m and μ is the transition dipole moment.

(b) In the *extended dipole* model, the transition dipole moment μ is replaced by two opposite charges $+q$ and $-q$ at a distance l;[10] q and l are two unknown parameters with no other condition than $ql = \mu$. Although this approximation is better than that of the point dipole model, it is used only by few authors. The coupling calculated according to this model is the sum of four charge−charge electrostatic interactions. At long distance, the extended dipole is equivalent to the point dipole. At short distance, this model is a rather good approximation for strongly allowed transitions whereas it is a very crude approximation for weak transitions.[1] A dipole length of the order of the size of the chromophore is generally chosen. However, a good way to choose the dipole length consists of adjusting the value of l from the calculation of the electrostatic interactions as presented in section 6. In the case of columnar aggregates, the general formula for the calculation of the exciton coupling in the extended dipole approximation is given by eq 5 where q,l,R,μ and $V_{n,m}$ are in atomic units:

$$V_{n,m} = \frac{2q^2}{R}\left[\frac{1}{\sqrt{1+\frac{l^2}{2R^2}(1-\cos\theta_{n,m})}} - \frac{1}{\sqrt{1+\frac{l^2}{2R^2}(1+\cos\theta_{n,m})}}\right] \tag{5}$$

(c) In the *atomic transition charge distribution* model, already mentioned in section 3.2.1, the coupling is expressed as the sum of charge−charge interaction terms between all the atoms of the chromophore m and all the atoms of the chromophore n.

$$V_{n,m} = \sum_{i=1}^{Nat}\sum_{j=1}^{Nat}\frac{q_i^n\, q_j^m}{r_{i,j}} \tag{6}$$

$r_{i,j}$ is the interatomic distance between the atoms i and j and q_i^n is the charge of the atome i. This atomic transition charge distribution results from our quantum chemistry calculations and represents the transition electronic density:

$$\sum_{i=1}^{Nat} q_i^n = 0 \text{ and } \sum_{i=1}^{Nat} q_i^n\, \vec{r}_i^{\,n} = \vec{\mu} \tag{7}$$

where $\vec{\mu}$ denotes the transition dipole moment. The detail of the calculation of these atomic charges in the INDO formalism is described in a previous paper.[1] Two charge distributions ($q_i^{n,I}$) and ($q_i^{n,II}$) are used to represent the electronic density associated to a degenerate transition where I and II represent the two components of the transition. In the case of the $S_0 \rightarrow S_4$ transition of H1TT, the contribution of the atomic transition charges to the total CS-INDO-CIPSI transition dipole moment is equal to 93%, and consequently, the approximation of a multicentric monopole expansion is reasonable.

The common aim of these three models is to provide a convenient way to calculate the exciton coupling whose direct expression is a sum of two-electron integrals. A recent review of the various models used in the calculation of the exciton coupling is given in ref 32.

A property of the matrix diagonalization is largely used in this study: when all the matrix elements are divided by the same constant, then all the eigenvalues (E_k) are divided by this same constant but each eigenvector ($C_{k,n}^i$) remains unchanged. One can notice that when the transition moment is multiplied by a factor f, the exciton coupling is mutiplied by f^2 whatever the model used (eqs 4−6). In section 6, for the degenerate $S_0 \rightarrow S_4$ transition, we have multiplied each transition atomic charge resulting from the CS-INDO CIPSI calculation by a factor f in order to adjust the CS-INDO-CIPSI value of the transition dipole moment ($\mu = 10.89$ D) to the value found from the fit of the absorption spectrum ($\mu = 9.2$D).

3.2.3. Degree of Localization of the Eigenstates. According to the linear expression of the wave functions (eq 1), the relative contribution of each chromophore n in the description of the total wave function $|k\rangle$, can be calculated from the square of the coefficient $(C_{k,n})^2$. This is a very common way to identify the nature of the wave functions in quantum chemistry. By sorting the localized configurations whose contribution is larger than a certain threshold, one can determine the number of chromophores L_k involved in the excitation of the eigenstate k. This resulting L_k number depends on the threshold value: the larger the threshold, the lower the L_k values.

TABLE 1: Excited State Properties Calculated by the CS-INDO-CIPSI Method

		H1TT		H1OT	
transition	symmetry	energy/cm^{-1}	μ/D	energy/cm^{-1}	μ/D
$S_0 \rightarrow S_1$	A'_1	27 700	0	28 800	0
$S_0 \rightarrow S_2$	A'_2	32 400	0	33 600	0
$S_0 \rightarrow S_3$	E′	32 900	5.77	34 600	5.60
$S_0 \rightarrow S_4$	E′	36 800	10.89	39 100	10.45
$S_0 \rightarrow S_5$	E′	39 300	0.92	41 400	1.19

Another way to define the number of chromophores participating in a given eigenstate k is to use the empirical parameter L_k defined as the inverse ratio of the sum of the fourth power of the coefficients.[6−8]

$$L_k = 1/\sum_{n=1}^{N}(C_{k,n})^4 \quad (8)$$

L_k is equal to N for a totally delocalized eigenstate (all the coefficients equal to $N^{-1/2}$), and it is equal to 1 for a single-site localized eigenstate. When the molecular electronic states are degenerate it is easy to show that eq 8 becomes

$$L_k = 1/\sum_{n=1}^{N}[(C^{I}_{k,n})^2 + (C^{II}_{k,n})^2]^2 \quad (9)$$

where $C^{I}_{k,n}$ and $C^{II}_{k,n}$ denote the two coefficients corresponding to the chromophore n in the description of the electronic transition.

From a comparative study of these two methods, in the case of H1TT columnar aggregates, the following conclusions were drawn, using either the square of an coefficients with a certain threshold or eqs 8 and 9. First, when the eigenstate is localized on a moderate number of chromophores (less than 20% of the total number), the two methods are equivalent and eqs 8 and 9 give a good estimation of the number of chromophores involved in the excitation. On the other hand, for largely delocalized eigenstates, with both methods it becomes difficult to precisely estimate the number of participating chromophores, since all the coefficients are very small. The L_k value corresponding to the eigenstate bearing the oscillator strength (noted $L_{k,abs}$) found from eqs 8 and 9 for an aggregate of 60 molecules is 43. This value can be compared to the theoretical value ($L_k = N = 60$) corresponding to an "equally" delocalized eigenstate. Actually, the ratio $L_{k,abs}/N$ decreases when N increases. As an example, $L_{k,abs}/N$ is respectively equal to 1, 0.78, 0.71, and 0.70 when N is equal to 2, 15, 60, and 200.

4. Properties of "Isolated" Chromophores

Table 1 shows the properties of the lowest energy singlet−singlet transitions calculated by the CS-INDO-CIPSI method for H1OT and H1TT. For both compounds, the transitions $S_0 \rightarrow S_1$ and $S_0 \rightarrow S_2$ are symmetry forbidden whereas $S_0 \rightarrow S_3$, $S_0 \rightarrow S_4$, and $S_0 \rightarrow S_5$ are symmetry allowed and degenerate. The two components of a degenerate transition are orthogonal and their vectorial sum, given in Table 1, corresponds to the experimental transition moment. $S_0 \rightarrow S_4$ is the most intense transition (Table 1). The transition energies calculated for H1TT are lower than those calculated for H1OT. This difference is ca. 1100 cm^{-1} for the three lowest in energy transitions and ca. 2200 cm^{-1} for the highest ones (Table 1).

The electronic absorption spectrum of H6TT in *n*-heptane (10^{-6} M) is red-shifted and less structured than the H5OT one (Figure 2). In light of our theoretical calculations, the absorption spectra are decomposed according to a vibronic progression model. The position of the peaks corresponding to $S_0 \rightarrow S_1$ (lowest in energy peak) and $S_0 \rightarrow S_4$ (most intense peak) are easily determined on the spectra whereas the energies of the other transitions are derived through a fitting procedure based on the results of the quantum chemistry calculations. For this purpose, a commercial software (Peak-Fit 4.0) is used. Each transition $S_0 \rightarrow S_i$ is simulated by the sum of N_i Gaussian bands with the same bandwidth W_i. N_i is fixed, whereas W_i, the energy at the maximum $\bar{\nu}_{(0-0)}$, and the amplitude of each Gaussian band are considered as fitting parameters. The minimum number of Gaussians giving a good fit is used. The H5OT spectrum is fitted first, because the vibronic progressions are more easily assigned on it. Then, the H6TT spectrum is fitted using the same number of gaussians as that found for H5OT. This is reasonable since electronic excitations are mainly localized on the aromatic core. Therefore, the active vibronic progressions are not expected to be related to peripheral groups (alkylthio or alkyloxy). The results of the fits are presented in Table 2.

TABLE 2: Decomposition of the Absorption Spectra of H6TT and H5OT in *n*-Heptane into Gaussian Bands According to a Model of Vibronic Progression (Figure 2)[d]

compound	transition	N_i	W_i/ cm^1	$\bar{\nu}_{(0-0)}$/ cm^{-1}	$\Delta\bar{\nu}$/ cm^{-1}	μ/D
H6TT	$S_0 \rightarrow S_1$	2	900	25400	1280	1.4[a]
	$S_0 \rightarrow S_2$	1	1360	28100[c]		2.1[b]
	$S_0 \rightarrow S_3$	3	1280	29100[c]	1180, 970	6.2[b]
	$S_0 \rightarrow S_4$	4	1400	32400	1320, 1310, 1310	9.6[a]
H5OT	$S_0 \rightarrow S_1$	2	700	27900	1050	1.0[a]
	$S_0 \rightarrow S_2$	1	840	30100[c]		1.1[b]
	$S_0 \rightarrow S_3$	3	1640	31300[c]	1460, 1660	5.7[b]
	$S_0 \rightarrow S_4$	4	1200	36000	1330, 1280, 1280	9.2[a]

[a] Estimated error: 10%. [b] Estimated error: 50%. [c] Estimated error: ±1000 cm^{-1}; the errors are due to the fact that somewhat different N_i values give acceptable fits. [d] N_i: number of gaussian bands. W_i: Gaussian bandwidth (fwhm). $\bar{\nu}_{(0-0)}$: energy of the first Gaussian band. $\Delta\bar{\nu}$: energy separation between two succesive gaussian bands. The transition dipole moment (μ) is determined from the sum of the areas $\int \epsilon(\bar{\nu})d\bar{\nu}$ beneath the N_i Gaussian according to the equation $\mu^2 = 9.166 \times 10^{-3} \int \epsilon(\bar{\nu})d\bar{\nu}/\bar{\nu}$.

The transition moments corresponding to $S_0 \rightarrow S_1$ and $S_0 \rightarrow S_2$ are higher for H6TT than for H5OT (Table 2). The oscillator strength of symmetry forbidden transitions is due to vibronic coupling with allowed transitions. The smaller the energy difference between the allowed and the forbidden transition, the higher the oscillator strength acquired by the latter.[33] The energy difference between the peaks corresponding to $S_0 \rightarrow S_1$ and $S_0 \rightarrow S_4$ is bigger for H5OT (8100 cm^{-1}) than for H6TT (7000 cm^{-1}). This could explain why the $S_0 \rightarrow S_1$ and $S_0 \rightarrow S_2$ transitions moments are larger for the thio derivative than for the oxygen derivative. Another origin for the oscillator strength of the studied hexasubstituted triphenylenes is a symmetry break because of a nonsymmetric arrangement of the side groups.[1]

The absorption spectra of H6TT show very weak solvatochromism, as reported for H5OT.[1] For both compounds, the largest shift is found between the absorption spectra recorded for *n*-heptane and dichloromethane solutions. It is about 3 times larger for $S_0 \rightarrow S_4$ (200 cm^{-1}) than that for $S_0 \rightarrow S_1$ (70 cm^{-1}). Larger variations of the $S_0 \rightarrow S_4$ excitation energy compared to the $S_0 \rightarrow S_1$ one, within columnar aggregates of H1OT, were also shown from a calculation of the electrostatic interaction energy (Figure 9 in ref 9). This remark will be used in section 7.

Similarly to the absorption spectra, the H6TT fluorescence spectra are also red-shifted and less structured than those of

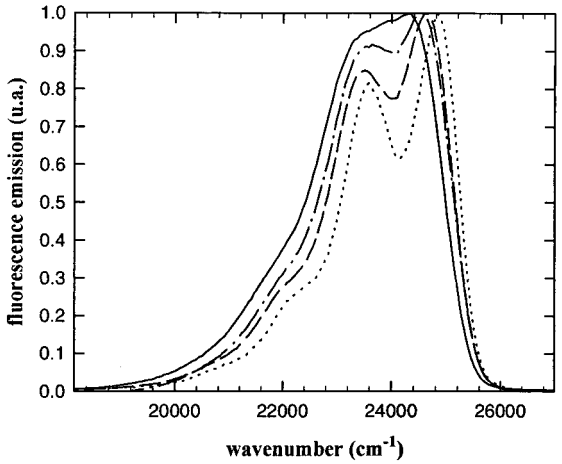

Figure 3. Fluorescence spectra of H6TT in *n*-heptane (···), diethyl ether (− −), ethanol (−·−) and dichloromethane (—); $\bar{\nu}_{ex}$ = 29000 cm^{-1}.

TABLE 3: Comparison of the Properties of H6TT and H5OT in Dichloromethane

compound	τ_f/ns[a]	Φ	τ_{rad}/ns	k_{rad}/s^{-1}	k_{nrad}/s^{-1}
H6TT	0.64	0.019[b]	34	2.9×10^7	1.5×10^9
H5OT	7.9	0.060[c]	120	8.3×10^6	1.2×10^8

[a] $\bar{\nu}_{ex}$: 33300 cm^{-1}. [b] $\bar{\nu}_{ex}$: 29000 cm^{-1}. [c] $\bar{\nu}_{ex}$: 25000 cm^{-1}.

H5OT. Their profile varies with the solvent (Figure 3), as reported for other aromatic chromophores.[34] The fluorescence properties of H6TT and H5OT in dichloromethane are compared in Table 3. The fluorescence lifetime (τ_f = 0.64 ns) and the fluorescence quantum yield (Φ = 0.019) of H6TT are both smaller than those of H5OT (τ_f = 7.9 ns, Φ = 0.06). The radiative lifetime, determined as $\tau_{rad} = \tau_f/\Phi$, is much shorter (34 ns) for H6TT than that for H5OT (120 ns), in agreement with the values of the transition moments derived from the absorption spectra. Moreover, the nonradiative rate constant, $k_{nrad} = k_{rad}(1 - \Phi)/\Phi$, of H6TT is 12 times higher than that of H5OT.

The radiative lifetime determined from the fluorescence lifetime and quantum yield measurements ($\tau_{rad} = \tau_f/\Phi$) can be compared to the τ_{rad} determined via the Strickler Berg formula.[35] In the latter case, τ_{rad} depends on the number of Gaussian bands attributed to $S_0 \rightarrow S_1$ in the decomposition of the absorption spectra. If N_1 is equal to 2, τ_{rad} is found to be 110 and 50 ns for H5OT and H6TT, respectively, in good agreement with the values reported in the previous paragraph. In contrast, when N_1 is equal to 1, much higher τ_{rad} values are found (495 ns for H5OT and 147 ns for H6TT). Consequently, the attribution of two Gaussians to $S_0 \rightarrow S_1$ is correct and is in agreement with the observation of a vibrational progression in fluorescence.

Finally, we remark by comparing the values in Tables 1 and 2 that quantum chemistry calculations provide a good description of the properties of "isolated" chromophores. Therefore, it is reasonable to use the atomic transition charge distribution calculated according to the same method in order to determine the exciton coupling (section 6).

5. Thin Film Properties

The absorption profile of thin films (Figure 4) depends on the phase. The crystalline phase spectra exhibit two shoulders, at ca. 31000 and 36000 cm^{-1}. The absorption maxima of the four H6TT neat phases are blue-shifted with respect to the solution spectra. We explain the observed blue shift of the

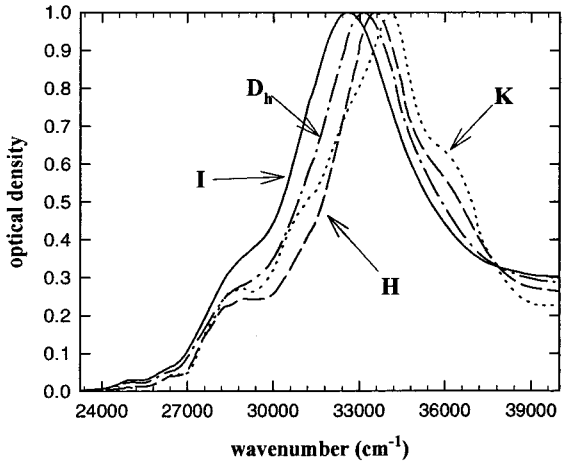

Figure 4. Absorption spectra recorded for thin films (<0.2 μm) of H6TT. Crystalline phase K at 40 °C (···), hexagonal phase H at 70 °C (− −), columnar liquid crystalline phase D_h at 90 °C (−·−), isotropic phase I at 120 °C (—).

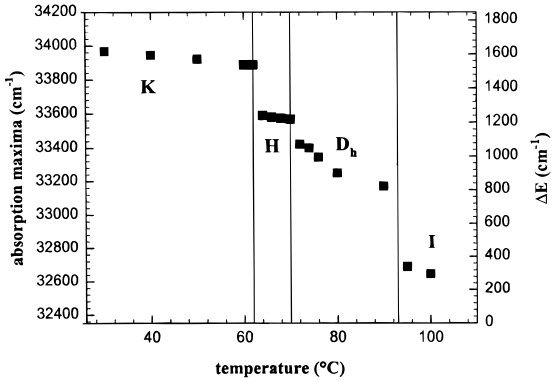

Figure 5. Temperature dependence of the absorption maximum determined for thin films (<0.2 μm) of H6TT. The scale on the right represents the energy difference (ΔE) with respect to the absorption maximum of H6TT in *n*-heptane.

absorption maximum corresponding to the strong $S_0 \rightarrow S_4$ electronic transition (μ = 9.6 D, Table 2), by the existence of strong exciton interactions leading to collective excited states. We note ΔE the difference in energy between the absorption maxima of thin films and *n*-heptane solutions. Within the temperature domain of each phase, ΔE decreases slowly with increasing temperature (T) and the largest $\Delta E/T$ slope is found for D_h (Figure 5). At each phase transition, a jump in ΔE is found: 320 cm^{-1} at the K → H, 160 cm^{-1} at the H → D_h, and 460 cm^{-1} at the D_h → I. The ΔE values of the four neat phases of the thio derivative H6TT are smaller than that of the D_h phase of the oxygen derivative H5OT (2000 cm^{-1}). Unlikely to what is found for H6TT (Figure 5), the ΔE value observed for the D_h phase of H5OT remains constant over its whole temperature domain (342−395 K). The temperature dependence of ΔE will be discussed in section 7.

Figure 6 shows the red edge of the absorption spectra obtained for the K, H, and D_h phases of H6TT. Using nonoriented films (macroscopically random orientation of microdomaines) of known thickness (section 2.2), we found that the Beer−Lambert law is obeyed. Thus, the molar absorption coefficient can be determined provided that the chromophore concentration is known. The molar concentration is calculated from the structural data provided by X-ray diffraction measurements taking into account the number of molecules per unit cell (4 for K, 3 for H and D_h) and the dimensions of the unit cell which

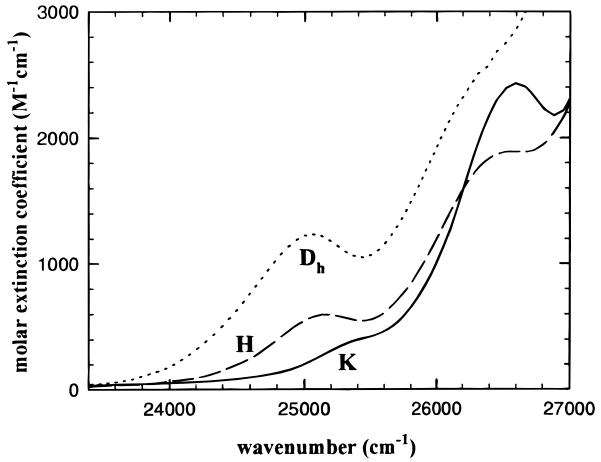

Figure 6. Molar extinction coefficient in the red edge of the absorption spectra of H6TT thin films. Crystalline phase K (—), hexagonal phase H (– –), columnar liquid crystalline phase D_h (•••).

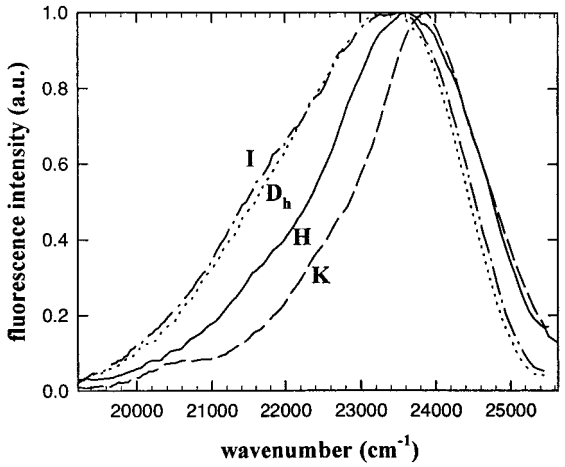

Figure 7. Fluorescence spectra of H6TT thin films; $\bar{\nu}_{ex} = 29\,000$ cm^{-1}. Crystalline phase K at 40 °C (– –), hexagonal phase H at 70 °C (—), columnar liquid crystalline phase D_h at 90 °C (•••), isotropic phase I at 120 °C (–•–).

is temperature dependent (1399 Å^3 for K at 40 °C, 1483 Å^3 for H at 70 °C, and 1509 Å^3 for D_h at 120 °C).[15,16]

The absorption bands shown in Figure 6, mainly correspond to the $S_0 \rightarrow S_1$ transition and can be decomposed in two Gaussians, as in the case of *n*-heptane solutions. Within the temperature domain of each phase, the positions of these bands are temperature independent. Going from K to H, the position of the $\bar{\nu}(0-0)$ band changes from 25650 to 25100 cm^{-1} and it is shifted to 25050 cm^{-1} upon the $H \rightarrow D_h$ transition. For $S_0 \rightarrow S_1$, being a symmetry forbidden electronic transition, molecular aggregation is not expected to lead to spectral shift associated to strong dipolar coupling (section 3.2.1). Therefore, we attribute the difference in the $\bar{\nu}(0-0)$ energy observed between the neat phases and the *n*-heptane solutions (250 cm^{-1} blue shift for K, 300 and 350 cm^{-1} red shift for H and D_h) to different strength of intermolecular forces. As explained in section 3.2.1, the predominant forces acting among triphenylene chromophores are the dispersion ones, which are always attractive. They are larger for the excited state than for the ground state leading to a red shift of the absorption of condensed phases with respect to isolated chromophores. Since they vary as $1/R$,[6] the closer the interatomic distances between neighboring molecules, the strongest the interaction. This explains the hypsochromic shift of $S_0 \rightarrow S_1$ observed in Figure 6 for the monoclinic K phase (average stacking distance: 3.9 Å) compared to the columnar hexagonal H phase (stacking distance: 3.6 Å).

The value of the $S_0 \rightarrow S_1$ transition moment is the same (1.3 ± 0.1 D) for the two solid phases, K and H, of H6TT and close to that determined for solutions (1.4 ± 0.1 D). Going from the solid H phase to the liquid crystalline D_h phase, the transition moment increases from 1.3 ± 0.1 D to 2.0 ± 0.4 D. This behavior characterizes only the thio derivative, since no noticeable change in the value of the $S_0 \rightarrow S_1$ transition moment is observed upon the $K \rightarrow D_h$ phase transition of H5OT. We are tempted to assign it to a symmetry break due to deformation of the C–S bonds, which are weaker than the C–O bonds. Such a deformation could be induced by structural fluctuations typical of columnar liquid crystals: column bending, lattice dilatation, or compression.[36]

The fluorescence spectra of thin films are all red shifted with respect to the solution spectra (Figure 7). The emission maximum is constant within the temperature domain of each phase but it changes abruptly upon the phase transitions (Figure 8a). The higher the temperature, the lower the energy of the

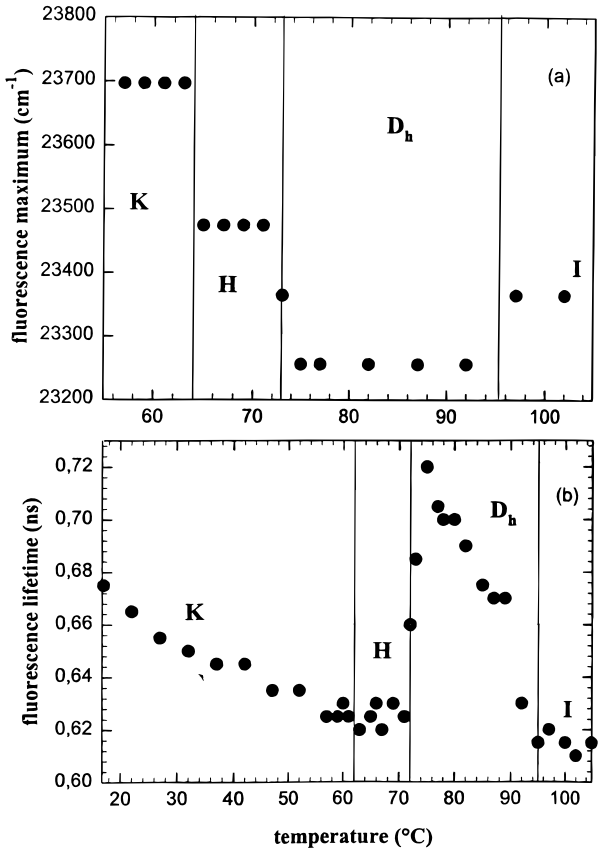

Figure 8. Temperature dependence of (a) the fluorescence maximum ($\nu_{ex} = 29000$ cm^{-1}) and (b) the fluorescence lifetime ($\bar{\nu}_{ex} = 33300$ cm^{-1}) of H6TT thin films.

emisssion maximum (23700, 23470, and 23240 cm^{-1} respectively, for K, H, and D_h) with the exception of the isotropic phase spectra whose maxima appear at 100 cm^{-1} higher energy than those of the D_h spectra. The spectrum width (fwhm) increases when going from K (1900 cm^{-1}) to H (2500 cm^{-1}) and then to D_h (2900 cm^{-1}). The spectra of the D_h and I phases are practically identical. The Stokes shift found for the neat phases (1900, 1600, 1800, and 1700 cm^{-1} for K, H, D_h, and I, respectively) is about 3 times larger than that determined for spectra of *n*-heptane solutions (600 cm^{-1}). Such a behavior could be explained by an interaction between the localized S_1 state and a higher in energy intermolecular charge transfer

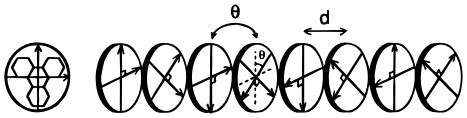

Figure 9. Schematic representation of the columnar aggregates considered in the numerical calculations. The aromatic cores are all parallel and their centers are located on the same axis. *d* denotes the stacking distance. Each molecule is rotated with respect to its neighbor by an angle θ.

state,[29,30] leading to excimer-like emission. However, both the width of the fluorescence spectra and the Stokes shift, although much larger than the monomer ones, are smaller than those found for typical excimers.[38,39] Consequently, fluorescence should arise from weakly bound excimers.

The fluoresence decays recorded for the four neat phases of H6TT can be fitted by a single exponential, and the corresponding lifetime is of the same order of magnitude as that of solutions. The temperature dependence of the fluorescence lifetime is shown Figure 8b. For the phases K, D_h, and I, it decreases with increasing temperature while it remains constant for H. The lifetimes found for D_h are longer than those found for all the other phases. The increased fluorescence lifetime and width of the emission band in the columnar D_h phase, compared to those observed for the columnar H phase, show exciton formation is favored by the disorder in the columnar stacks.

6. Numerical Study of the Exciton States

In this Section we are interested in the exciton states of triphenylene columnar aggregates built on the S_4 state which is degenerate and corresponds to the maximum of the absorption spectra (Figures 2 and 4). In our study, we assume a static distribution of molecular orientations. This hypothesis is quite reasonable since molecular motions in liquid crystals occur in the pico- or nanosecond time scale and are therefore much slower than the time of intermolecular excitation transfer.[39] First, we present some details about the system for which calculations are performed. Then, we examine how different approximations used to calculate the off-diagonal terms in the Hamiltonian matrix affect the eigenstate properties. These approximations, developed in section 3.2.2, concern the number of interacting neighbors (nearest neighbor or long-range interactions), the model used for the calculation of the exciton coupling (point dipole, extended dipole, atomic transition charge distribution), and the use of a dielectric constant. Finally, we study the influence of disorder on the eigenstate properties. To find out any particular behavior due to the degeneracy of molecular excited states, we perform our calculations for both degenerate and nondegenerate excited states.

6.1. Presentation of the System. We consider a columnar stack consisting of *N* H1TT molecules ($N = 2, 3, ..., 100$). Their aromatic cores are all parallel and their centers are located on the same axis (Figure 9). The stacking distance *d* is either constant equal to 3.6 Å or takes random values in the interval 3.4−3.8 Å (positional disorder). Each molecule is rotated with respect to its neighbor by an angle θ. The angle θ is either constant (helical structure), or takes random values in the interval 0°−360° (orientational disorder). Orientational and positional disorder are studied separately. When we study the influence of disorder, we report the results obtained for 20 individual random configurations but not the average values.

All diagonal terms are set equal to zero (section 3.2.2). To compare the results of the calculations with the experimental absorption spectra (section 7), we use the $S_0 \rightarrow S_4$ transition

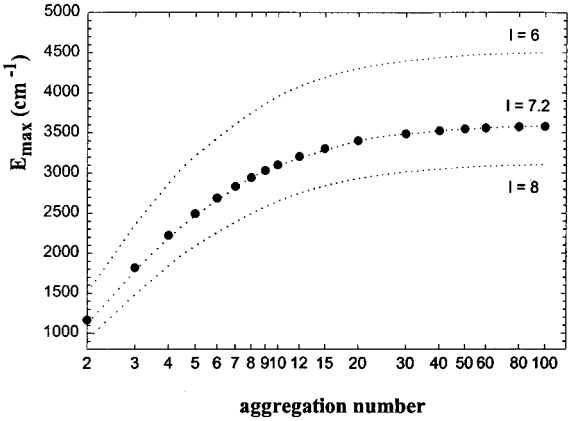

Figure 10. Energy of the upper eigenstate (E_{max}) as a function of the aggregation number. Columnar helical aggregates of H1TT ($\theta = 45°$). Degenerate molecular electronic transition ($\mu_1 = \mu_2 = 6.8$ D). The exciton coupling is calculated including long-range interactions and using two different models: the atomic charge distribution model (closed circles) and the extended dipole model (dotted lines), and *l* denotes the length (6, 7.2, and 8 Å) of the extended dipole.

dipole moment determined from the fit of the absorption spectra ($\mu = 9.6$ D) rather than the value obtained from quantum chemistry calculations ($\mu = 10.9$ D). The two components of the degenerate transition are $\mu_1 = \mu_2 = 9.6/\sqrt{2} = 6.8$ D. When the properties of eigenstates built on degenerate molecular states are compared to those built on nondegenerate molecular states (section 6.3), we consider that the transition moment of the nondegenerate transition is equal to the total transition moment of the degenerate one ($\mu = 9.6$ D). In this way, both types of transition could correspond to the same experimental absorption band. For an aggregate of *N* molecules, the dimension of the exciton matrix is ($2N \times 2N$) when the transition is degenerate, instead of ($N \times N$) for a nondegenerate transition.

6.2. Approximations in the Calculation of the Off-Diagonal Terms. In this subsection, columnar aggregates having the structural characteristics of the helical H phase are considered. Whatever the level of approximation, when the molecular states are degenerate, all eigenstates are degenerate and the oscillator strength is born by the upper one. Therefore, we mainly focus on the energy of the highest eigenstate (E_{max}) since it can be related to the experimental absorption spectra. We are also interested in the "symmetry" of the exciton band, that is the position of the upper (E_{max}) and lower (E_{min}) eigenstates with respect to the excited-state energy of noninteracting chromophores. To this end, we calculate the ratio $E_{max}/(E_{max} - E_{min})$.

Figure 10 shows E_{max}, calculated using the atomic charge distribution model and including long-range interactions, as a function of the aggregation number. E_{max} increases with the aggregation number and remains practically constant for *N* greater than 60. It can be seen in Figure 11, that interactions involving up to the sixth neighbor must be taken into account in order to have an error smaller than 200 cm^{-1}. If only nearest neighbor interactions are taken into account, the position of E_{max} is underestimated by ca. 35% for large aggregates. The "symmetry" of the exciton band also depends on the number of interacting chromophores. In the nearest neighbor approximation, E_{max} and E_{min} are symmetrically distributed around the zero level. When all the interactions are considered, the positions of all the eigenstates are shifted to higher energy but the density of states in the lower part of the exciton band increases, whereas it decreases in the upper part. $E_{max}/(E_{max} - E_{min})$ becomes 0.66 instead of 0.50. A similar trend is reported

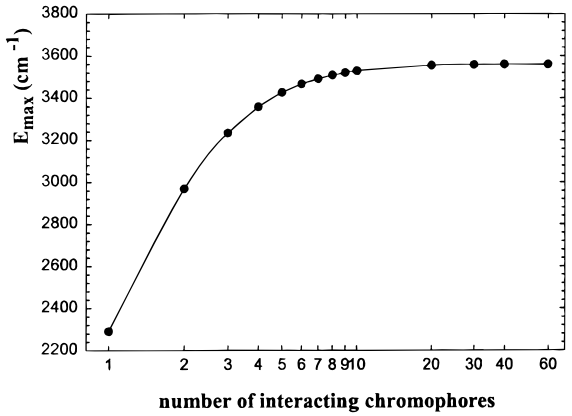

Figure 11. Energy of the upper eigenstate (E_{max}) as a function of the number of interacting chromophores. Columnar helical aggregates of H1TT ($N = 60$, $\theta = 45°$, degenerate molecular electronic transition: $\mu_1 = \mu_2 = 6.8$ D). The exciton coupling is calculated according to the atomic charge distribution model including long range interactions.

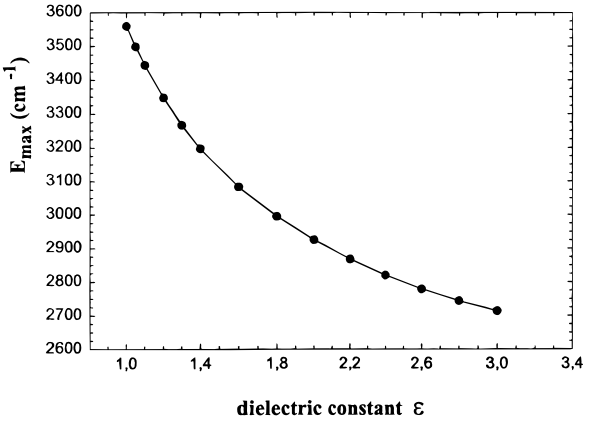

Figure 12. Energy of the upper eigenstate (E_{max}) as a function of the dielectric constant ϵ_∞ taken into account in the calculation of the long-range coupling $V_{n,n+i}$ with $i > 1$. For nearest neighbor coupling ($V_{n,n+1}$), ϵ_∞ is taken equal to 1. Columnar helical aggregates of H1TT ($N = 60$, $\theta = 45°$, degenerate molecular electronic transition: $\mu_1 = \mu_2 = 6.8$ D). The exciton coupling is calculated according to the atomic charge distribution model.

for J aggregates where the oscillator strength is born by the lowest eigenstate: when all interactions are taken into account, E_{min} is shifted to lower energy and the exciton band becomes less symmetric.[7]

We tested the extended dipole approximation for various lengths (l) of the extended dipole. Figure 10 shows that E_{max} calculated for $l = 7.2$ Å matches that found using the atomic transition charge distribution model. It is worth mentioning that the curve VR^3 as a function of R obtained according to the atomic transition charge distribution model can be fitted using the same length ($l = 7.2$ Å) of the extended dipole (Figure 10 in ref 1). We remark that the latter value corresponds to the diameter of the disk defined by the triphenylene aromatic core alone and not of the disk including also the six sulfur atoms (10 Å). This value of 7.2 Å is much longer than the distance between the barycenters of the positive and negative charges (3 Å) associated to the degenerate $S_0 \rightarrow S_4$ transition from quantum chemistry calculations (section 3.2.2). When l decreases, the exciton coupling increases (eq 5), and consequently, E_{max} increases. Moreover, the exciton band becomes more symmetric (Table 4) showing that the "symmetry" of the exciton band depends not only on the number of interacting chromophores but also on their "size".

Some authors using the point dipole or the extended dipole approximation divide the exciton coupling by the dielectric constant ϵ_∞ of the medium. As a result, E_{max} is divided by the same ϵ_∞ value (section 3.2.2). The dielectric constant is supposed to account for the quasi-instantaneous polarization of the electronic clouds in the medium upon light excitation and is equal to the square of the refractive index. Typical ϵ_∞ values of 2.5−2.7 are used.[10,40−42] The dielectric constant is a macroscopic property of the medium which has no meaning at a molecular level. The polarization of the electronic clouds is in principle taken into account in a complete quantum chemical description of the overall system. However, a complete description has not been performed so far for systems consisting of a big number of large molecules. In order to roughly simulate the distance dependence of this effect, we consider that ϵ_∞ is equal to one for nearest neighbor coupling ($V_{n,n+1}$) since no molecules are intercalated in between. For long distance coupling ($V_{n,n+i}$ with $i > 1$), ϵ_∞ is given a constant value, ranging from 1.1 to 3.0. We are conscious that this is a further approximation but it seems to us more appropriate than the use of a uniform value of dielectric constant. The introduction of a dielectric constant only for long-range interactions leads to a decrease of E_{max} (Figure 12) and makes the exciton band more symmetric (Table 4). When ϵ_∞ tends to very high values, the structure of the exciton matrix tends to that of a Hückel matrix and E_{max} tends toward the value (2290 cm^{-1}) obtained considering only nearest neighbor interactions (Table 4 and Figure 12).

General conclusions can be drawn from Table 4, where E_{max} and the "symmetry" of the exciton band, calculated using different approximations, are gathered. In the point dipole approximation, E_{max} is largely overestimated with respect to the values calculated according to the atomic transition charge distribution model. Typically, E_{max} is 4.2, 3.5, or 3.3 times bigger, for aggregation numbers equal to 2, 10, or 100, respectively. Conversely, within the atomic transition charge ditribution model, E_{max} is underestimated by 35% in the nearest neighbor approximation compared to the case where all the coupling are taken into consideration. This means that the error made using the point dipole approximation is much bigger than that made following the nearest neighbor approximation. Table 4 shows that E_{max} may vary by 1 order of magnitude depending on the approximation level. It is worth noticing that the errors made by different approximations may compensate each other. For example, the point dipole model with the nearest neighbor approximation leads to a E_{max} value of 9926 cm^{-1}, which can be reduced to the value found using the atomic transition charge distribution model (3559 cm^{-1}) by the introduction of a dielectric constant equal to 2.8. In that case, although the E_{max} value is artificially corrected, the error made in the "symmetry" of the exciton band remains (Table 4).

6.3. Influence of Disorder: Comparison of Degenerate and Nondegenerate States. We examine how off-diagonal disorder affects E_{max} and the degree of localization of the exciton states. For this purpose, columnar aggregates consisting of sixty molecules are studied. We directly correlate off-diagonal disorder to structural disorder, orientational and positional, by changing the coordinates of the molecules within the aggregate. The off-diagonal terms are calculated using the atomic transition charge distribution model including long range interactions without taking any dielectric constant into account.

The effect of diagonal disorder on E_{max} is only briefly discussed because we cannot correlate diagonal disorder to structural disorder. As explained in section 3.2.1, the interaction energy among triphenylene chromophores is governed by

TABLE 4: Energy of the Upper Eigenstate E_{max} and "Symmetry" of the Exciton Band $E_{max}/(E_{max} - E_{min})$ Calculated Using Different Levels of Approximation[a]

	approximation	E_{max} /cm^{-1}	$E_{max}/(E_{max} - E_{min})$
point dipole	nearest neighbor interactions	9926	0.50
	long-range interactions	11896	0.57
	long-range interactions, $\epsilon_{n(n+i)} = 2.5$ for all i	4758	0.57
	long-range interactions, $\epsilon_{n(n+i)} = 2.5$, for $i > 1$	10713	0.53
atomic transition charge distribution	nearest neighbor interactions	2290	0.50
	long-range interactions	3559	0.66
	long-range interactions, $\epsilon_{n(n+i)} = 2.5$ for all i	1424	0.66
	long-range interactions, $\epsilon_{n(n+i)} = 2.5$, for $i > 1$	2797	0.57
extended dipole	long-range interactions/$l = 3$ Å	8285	0.59
	long-range interactions/$l = 7.2$ Å	3560	0.68
	long-range interactions/$l = 10$ Å	2228	0.74

[a] E_{min} denotes the energy of the lowest eigenstate. $\epsilon_{n(n+i)}$: dielectric constant used in the calculation of the exciton coupling for the chromophores n and $n + i$; its value is reported only when it is different than one. Columnar aggregates consist of 60 H1TT molecules and have the geometrical characteristics of the helical H phase. Degenerate transition ($\mu_1 = \mu_2 = 6.8$ D).

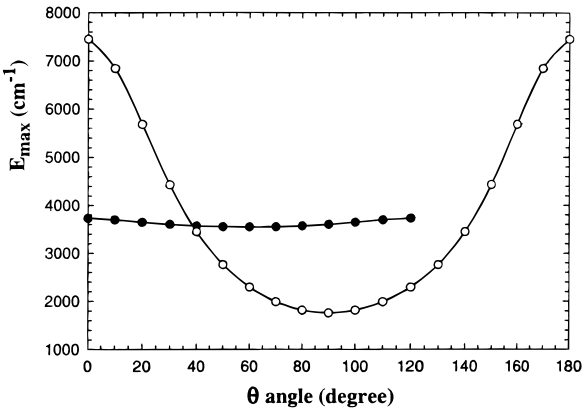

Figure 13. Energy of the upper eigenstate (E_{max}) of columnar helical aggregates of H1TT ($N = 60$) as a function of the angle θ. Exciton coupling is calculated according to the atomic charge distribution model including long range interactions. Closed circles: degenerate transition ($\mu_1 = \mu_2 = 6.8$ D). Open circles: nondegenerate transition ($\mu = 9.6$ D).

dispersion forces which cannot be calculated with acceptable accuracy for the excited states. Therefore, diagonal disorder is simulated by setting random numbers directly to the diagonal terms of the Hamiltonian matrix. The two types of disorder are studied separately. When off-diagonal disorder is studied, the diagonal terms are zero, whereas when diagonal disorder is introduced, we consider aggregates having the geometrical configuration of the helical H phase.

Figure 13 illustrates the dependence of E_{max} on the θ angle of a helical stack for degenerate and nondegenerate transitions. The difference between the two patterns is quite striking. For nondegenerate transitions, changes in θ may induce variations on E_{max} as large as 5700 cm^{-1}, whereas for degenerate transitions, changes in θ have only a weak effect on E_{max}, lower than 250 cm^{-1} (Table 5). In the case of degenerate transitions, the variations of E_{max} are equal to 5%. When the extended dipole model is used instead of the atomic transition charge distribution model, the magnitude of these variations depends on the dipole length. They are 2%, 13%, and 19% when l is equal to 3, 7.2, and 10 Å, respectively.

For degenerate molecular states, the oscillator strength is always born by the upper eigenstate whereas, for nondegenerate ones, absorption toward the five highest eigenstates may be important. The variation of the localization index L_k (section 3.2.3) found for the eigenstates of helical aggregates as a function of θ is presented in Table 5. In the case of degenerate molecular transitions, we found that, whatever the θ value, the upper eigenstate is always largely delocalized ($L_{k,abs} = 43$). The other eigenstates are also extended; their L_k values range between 37 and 47. In the case of nondegenerate transitions, high values of $L_{k,abs}$ (43) are also found for $\theta = 0°$; the minimum $L_{k,abs}$ value (28) is obtained for $\theta = 45°$. It is worth noticing that, for $\theta = 90,°$ despite the absence of nearest neighbor interactions, many of the eigenstates are largely delocalized as predicted in ref 5.

We tested the effect of orientational disorder by attributing random values to the angles θ. For degenerate transitions, the E_{max} values are located within the range of E_{max} found for helical aggregates (Table 5) and the variations are small (3635 ± 20 cm^{-1}). For nondegenerate transitions, the position of the upper eigenstate varies between 4400 and 6000 cm^{-1}. For nondegenerate states, the localization index decreases significantly, now ranging from 1 to 25. For degenerate states, the eigenstates located in the upper part of the exciton band remain largely delocalized (Table 5).

The results summarized in Table 5 clearly show that the

TABLE 5: Influence of Orientational Disorder on the Energy (E_{max}) of the Upper Eigenstate and the Localization Index (L_k) of the Eigenstates

type of molecular transition	chromophore orientation around the column axis	E_{max}/cm^{-1}	$L_{k,abs}$[a]	L_k[a]
degenerate	helical	[3550−3750]	43	[37−47]
	random	[3615−3655]	43	[37−48]
nondegenerate	helical	[1750−7450]	28 ($\theta = 45°$)[b]	[28−47]
			43 (θ=0° or 90°)[b]	
	random	[4400−6000]	10	[2−25]

[a] From eqs 8 and 9. [b] θ: angle between neighboring chromophores ranging from 0° to 360°. In helical aggregates, all angles θ are identical. [c] $L_{k,abs}$ denotes the localization index of the eigenstate bearing the oscillator strength. Columnar aggregates consisting of 60 H1TT molecules. The coupling is calculated according to the atomic transition charge distribution model including long-range interactions without considering any dielectric constant.

properties (E_{max} and L_k) of eigenstates built on degenerate molecular states are not very sensitive to off-diagonal disorder induced by orientational structural disorder. Indeed, when the molecular transitions are degenerate, there are four exciton interactions for each molecular pair. When the angle θ changes, two of them decrease while the two others increase, compensating each other.

Focusing on helical aggregates ($\theta = 45°$), we examine the influence of the stacking distance d (positional disorder) on the eigenstate properties. When the stacking is regular (d constant between 3.4 and 3.8 Å), E_{max} varies quasi linearly with d. A 0.1 Å increase of d leads to a decrease of E_{max} by ca. 150 cm^{-1} for degenerate or nondegenerate transitions. It is worth stressing that the influence of the stacking distance on E_{max} greatly depends on the model used in the calculation of the exciton coupling. For example, the variation calculated in the point dipole approximation are 7 times larger than that calculated in the atomic transition charge distribution approximation; a 0.1 Å increase of d leads to a decrease of E_{max} by ca. 1000 cm^{-1} both for degenerate or nondegenerate transitions. This happens because, in point dipole approximation, the coupling varies as $1/R^3$, whereas, in the atomic transition charge distribution model, it varies as $1/R$ at short distances.[1]

If the stacking is not regular and d varies randomly between 3.4 and 3.8 Å, it induces only small variations of E_{max}, 1.5% with respect to the value found for $d = 3.6$ Å. For the same positional disorder as above, the changes of E_{max} are much larger (15%) if the coupling is calculated in the point dipole approximation. This type of positional disorder does not affect the localization index.

With regard to diagonal disorder, we limited our study to only one type of calculation. We varied the diagonal terms by introducing random numbers ranging between -500 and 500 cm^{-1}. These energy fluctuations correspond to the width of the absorption band associated to the localized $S_0 \rightarrow S_1$ transition observed for the columnar H phase of H6TT (Figure 6). We found that in the presence of such diagonal disorder E_{max} is slightly blue-shifted. This shift is less than 100 cm^{-1} for degenerate molecular states and somewhat higher (ca. 200 cm^{-1}) for nondegenerate states.

7. Comparison between Experiment and Theory

Among the various calculated eigenstate properties, the only one which can be compared to an experimental observable is the energy of the upper eigenstate. We showed in section 6.2 that for degenerate molecular states, the oscillator strength is born by the upper eigenstate. Therefore, E_{max} is to be related to the maxima of absorption spectra. We cannot perform correct line shape analysis because the absorption bands of the neat phases are artificially broadened due to the nonuniform optical pathlength in very thin films. This apparent spectral broadening will be described quantitatively in a forthcoming communication.[43]

In section 5, we denoted by ΔE the difference in the absorption maxima of neat phases and *n*-heptane solutions. ΔE can be decomposed in two terms:

$$\Delta E = E_{exc} + \Delta E_{solv} \qquad (10)$$

where E_{exc} is the pure exciton shift which has to be compared to E_{max}. ΔE_{solv} is the difference in the energy of the localized $S_0 \rightarrow S_4$ transition of the studied triphenylene derivatives in *n*-heptane solution and in their neat phases, due to different intermolecular forces in these two different local environments.

TABLE 6: Comparison between Experiment and Theory[f]

	compound				
	HO5T (D_h)	H6TT (K)	H6TT (H)	H6TT (D_h)	H6TT (I)
ΔE^a	2000	1600	1250	1050−800	350
ΔE_{solv}	−900		−900	−1050	−900
E_{exc}	2900		2150	2100−1850	1250
$E_{max}{}^b$	3300[c]	*e*	3550[d]		

[a] From section 5. [b] Calculated according to the atomic transition charge distribution model including long-range interactions without taking any dielectric constant into account ($N = 60$). [c] Hhelical aggregates ($\theta = 30°$), molecular transition moment = 9.2 D. [d] Helical aggregates ($\theta = 45°$), molecular transition moment = 9.6 D. [e] E_{max} is not calculated for K because the structure is not columnar but monoclinic.[15] [f] ΔE is the difference in the absorption maxima of neat phases and *n*-heptane solutions. ΔE_{solv} is the energy difference of the molecular $S_0 \rightarrow S_4$ transition in neat phases and *n*-heptane solutions. $E_{exc} = \Delta E - \Delta E_{solv}$. E_{max} is the calculated energy of the upper eigenstate.

In general, ΔE_{solv} cannot be determined experimentaly and many authors consider that it is equal to zero.

In the particular case of triphenylene chromophores we can evaluate ΔE_{solv} by observing the position of the absorption band corresponding to the localized S_1 state. First, we found that this band is shifted only 50 cm^{-1} upon the H $\rightarrow$ D_h phase transition of H6TT with no further shift over the whole temperature domain of the D_h phases (section 5). This means that orientational and positional disorder do not affect significantly the excitation energy. Second, the position of the localized $S_0 \rightarrow S_1$ transition in the columnar phases is red-shifted by ca. 300 cm^{-1} with respect to its position found for *n*-heptane solutions. Third, the maximum solvatochromic shift observed for $S_0 \rightarrow S_4$ of both H5OT and H6TT is three times larger than that found for $S_0 \rightarrow S_1$ (section 4). Consequently, we estimate that the ΔE_{solv} for $S_0 \rightarrow S_4$ corresponding to a given columnar phase is about 3 times the ΔE_{solv} for $S_0 \rightarrow S_1$. These values, around 1000 cm^{-1} (Table 6), are not negligible compared to the observed spectral shifts ΔE.

The values of ΔE, ΔE_{solv}, and E_{exc} obtained from the eq 9 for the D_h phase of H5OT and three neat phases of H6TT are gathered in Table 6. The E_{max} values presented in the same table were calculated according to the atomic transition charge distribution model including long-range interactions without taking any dielectric constant into account. We considered helical aggregates having the structural characteristics of the columns in the corresponding phases. In order to check any possible intercolumnar interaction, we calculated E_{max} for two parallel aggregates located at 20−22 Å (intercolumnar distance in the neat phases) from each other. We obtained the same E_{max} value as for a single aggregate. Thus, the systems studied can be viewed as one-dimensional regarding to the eigenstate energy. The length of the columns is at least equal to the correlation length determined by X-ray diffraction measurements. The latter corresponds to 80 molecules for the D_h phase H5OT,[44] to 220 molecules for the H phase of H6TT, but only to four to eight molecules for the D_h phase of H6TT.[16] Therefore, the E_{max} values in Table 6, calculated for large aggregates, are given only for the D_h phase H5OT and H phase of H6TT.

We remark in Table 6 that the values of E_{exc} and E_{max} found for the D_h phase H5OT (2900 and 3300 cm^{-1}, respectively) are quite close. The 15% difference could be associated with the evaluation of ΔE_{solv} and the determination of the molecular transition moment through the fitting procedure described in section 4. As a matter of fact, an error of 10% in the determination of the transition moment from the experimental

absorption spectra (Table 2) induces an error of ca. 20% in E_{max} (section 3.2.2). In the case of H6TT helical phase, E_{max} exceeds E_{exc} by 70%. The position of E_{max} may be affected by interactions between Frenkel excitons and charge-transfer excitons,[29,30,45] neglected in our analysis of the exciton states. It would not be surprising that these interactions are stronger for H6TT compared to those of H5OT since charge transport in columnar phases is more efficient for the sulfur derivative.[46]

E_{exc} remains practically the same in both phases of H6TT (Table 6) being insensitive to the rotational and positional disorder. This behavior is in agreement with the results of our numerical calculations which revealed that this disorder does not affect the energy of the upper eigenstate, provided that it is built on degenerate molecular states. The E_{exc} of the D_h phase decreases slightly with increasing temperature; it has 90% of its initial value near the $D_h \rightarrow I$ transition. The correlation length of the columns being quite small for the D_h phase, it is possible that a temperature increase reduces the physical length of the columns. Figure 10 suggests that a 10% decrease in the E_{max} may be due to a reduction of the aggregation number from $N \geq 100$ to 12. Finally, the value of E_{exc} in the isotropic phase is still quite large (1250 cm^{-1}) indicating that even though long range order is lost in this phase, aggregates consisting of a few molecules ($N = 3-4$ according to Figure 10) persist. This finding is corroborated by the fluorescence spectra of the isotropic phase which resemble those of the D_h phase (Figure 7) and not of the solutions (Figure 3).

8. Summary and Conclusions

The main findings of the present work, where the properties of hexaalkylthiotriphenylenes were studied and compared to those of hexaalkyloxytriphenylenes, can be summarized as follows.

First, the isolated chromophores were studied. The properties of the lowest singlet excited states were calculated by the CS-INDO-CIPSI method. The results of these calculations showed that the absorption maximum corresponds to the degenerate $S_0 \rightarrow S_4$ transition whereas the lowest energy transition $S_0 \rightarrow S_1$ is symmetry forbidden. The absorption spectra of solutions were decomposed according to a model of vibronic progressions and the energy and the transition dipole moments of the four lowest transitions were determined. This spectral analysis revealed that the theoretically forbidden transitions of the thio derivative have larger dipole moments than those of the oxygen derivative. The fluorescence of the neat phases is attributed to weakly bound excimers. The most striking result is that the oscillator strength related to the lowest excited state increases by 40% when the liquid crystalline D_h phase is formed. This behavior is observed only for the thio derivative.

The properties of exciton states of aggregates having the structural characteristics of the columnar phases were calculated numerically. As a first step, we examined how different approximations made in the calculation of the off-diagonal terms in the Hamiltonian matrix affect the energy of the upper eigenstate and the "symmetry" of the exciton band. Taking as a reference the energy of the upper excited-state calculated using the atomic transition charge distribution model, we demonstrated that the error made using the point dipole model is much larger (+330%) and of opposite sign than that made by the nearest neighbor approximation (−35%). The extended dipole model may provide a good prediction of the spectral shift provided that its length is correctly adjusted. The "symmetry" of the exciton band depends both on the number of interacting chromophores and on their size. The absorption maximum, experimentally observed for the D_h phase of the oxygen derivative, is in good agreement with the value calculated using the atomic charge transition model without taking any dielectric constant into account (15% error). The agreement is not as good for the columnar phases of H6TT (70% error), possibly because of interactions between Frenkel excitons and charge-transfer excitons.

The effects of off-diagonal on the energy of the upper eigenstate and the degree of localization were also examined. We correlated off-diagonal disorder to structural disorder (orientational and positional) simulated by changing the coordinates of the molecules within the aggregate. Orientational disorder was found to have a dramatic effect on the energy and the localization extent of the upper eigenstate when it is built on nondegenerate states. In contrast, when the molecular states are degenerate, the eigenstate properties are practically almost unaffected by orientational disorder. For both types of molecular states, positional disorder has only a weak influence on the previously cited properties. The magnitude of the off-diagonal disorder induced by positional disorder was shown to depend largely on the model used in the calculation of the exciton coupling. The results of numerical calculations are in agreement with the experimental observations since, the absorption maxima of H6TT columnar phases hardly change upon the $H \rightarrow D_h$ phase transition inducing orientational and positional disorder.

This experimental and theoretical study of discotic triphenylenes allows us to draw general conclusions and foresee future developments. (i) The prediction of the absorption maxima corresponding to collective excited states is highly improved when the exciton coupling is calculated within the atomic charge distribution model. It would be interesting to extend this method to other systems which offer a larger number of observables which can be compared with the results of numerical calculations. Such observables may be the absorption line shape and also fluorescence related to exciton band (J-aggregates, phthalocyanine columnar phases, etc.). (ii) Our work showed that the degeneracy of molecular excited states make collective states much less sensitive to structural disorder. The question arises whether the same lack of sensitivity exists for other properties, like energy and charge transport, when degenerate states are involved. A study of excitation hopping, using Monte Carlo simulations, is underway.

Acknowledgment. This work has been performed within the framework of COST D4 Action (Project D4/0004/93). We thank Pr. H. Ringsdorf (University of Mainz, Germany) who initiated the synthesis of the studied compounds.

References and Notes

(1) Markovitsi, D.; Germain, A.; Millié, P.; Lécuyer, P.; Gallos, L.; Argyrakis, P.; Bengs, H.; Ringsdorf, H. *J. Phys. Chem.* **1995**, *99*, 1005.

(2) Davydov, A. S. *Theory of Molecular Excitons*; Plenum Press: New York, 1971.

(3) Rashba, E. I.; Sturge, M. D. *Excitons*; North-Holland Publishing Company: New York, 1982.

(4) It would be impossible to report all the studies dealing with the influence of disorder on electronic excitations. The few papers cited here[4−7] are those to which we refer later in the text.

(5) Economou, E. N.; Cohen, M. H. *Phys. Rev. B* **1971**, *4*, 396.

(6) Schreiber, M.; Toyozawa, Y. *J. Phys. Soc. Jpn.* **1982**, *51*, 1537.

(7) Fidder, H.; Knoester, J.; Wiersma, D. A. *J. Chem. Phys.* **1991**, *95*, 7880.

(8) Fidder, J.; Wiersma. D. A. *J. Phys. Chem.* **1993**, *97*, 11603.

(9) Murell, J. N.; Tanaka, *J. Mol. Phys.* **1964**, *7*, 364.

(10) Czikkleky, V.; Försterling, H. D.; Kuhn, H. *Chem. Phys. Lett.* **1970**, *6*, 207.

(11) Ecoffet, C.; Markovitsi, D.; Millié, P.; Lemaistre, J. P. *Chem. Phys.* **1993**, *177*, 629.
(12) Cornil, J.; Heeger, A. J.; Bredas, J. L. *Chem. Phys. Lett.* **1997**, *272*, 463.
(13) Gramsbergen, E. F.; Hoving, H. J.; de Jeu, W. H.; Praefcke, K.; Kohne, B. *Liq. Cryst.* **1986**, *1*, 397.
(14) Fontes, E.; Heiney, P. A.; de Jeu, W. H. *Phys. Rev. Lett*. **1988**, *61*, 1202.
(15) Heiney, P. A.; Fontes, E.; de Jeu, W. H.; Riera, A.; Caroll, P.; Smith III, A. B. *J. Phys.* **1989**, *50*, 461.
(16) Lee, W. K.; Heiney, P. A.; McCauley, J. P.; Smith, A. B., III *Mol. Cryst. Liq. Cryst.* **1991**, *198*, 273.
(17) Idziak, S. H.; Heiney, P. A.; McCauley, J. P., Jr.; Caroll P.; Smith, A. B., III *Mol. Cryst.*
(18) When our work was completed, we got to know an investigation of the H6TT properties in solution.[19] The experimental findings reported in ref 19 are in agreement with those found by us, but our analysis of the excited states based on quantum chemical calculations is somewhat different.
(19) Baunsgaard, D.; Larsen, M.; Harrit, N.; Frederiksen, J.; Wilbrandt, R.; Stapelfeldt, H. *J. Chem. Soc., Faraday Trans*. **1997**, *93*, 1893.
(20) Kohne, B.; Poules, W.; Praefcke, K. *Chem. Ztg*. **1983**, *108*, 113,.
(21) Boden, N.; Borner, R. C.; Bushby, R. J.; Cammidge, A. N.; Jesudason, M. V. *Liq. Cryst.* **1993**, *15*, 851.
(22) Velapoldi, R. A.; Mielenz, K. D. *Natl. Bur. Stand. (U.S.), Spec. Publi.* **1980**, 260.
(23) Germain, A.; Millié, P. *Chem. Phys.* **1997**, *219*, 265.
(24) Zehnacker, A.; Lahmani, F.; Bréhéret, E.; Desvergne, J. P.; Bouas-Laurent, H.; Germain, A.; Brenner, V.; Millié, P. *Chem. Phys*. **1996**, *208*, 243.
(25) Marguet, S.; Germain, A.; Millié, P. *Chem. Phys*. **1996**, *208*, 351.
(26) Stewart, J. J.; Seiler, F. J. MOPAC program, version 4.0; Research Laboratory, U. S. Air Force Academy: Colorado Spring, CO 80840, 1987.
(27) Huron, B.; Malrieu, J. P.; Rancurel, P. *J. Chem. Phys*. **1973**, *58*, 5745.
(28) Evangelisti, S.; Daudey, J. P.; Malrieu, J. P. *Chem. Phys.* **1983**, *75*, 91; *Liq. Cryst.* **1993**, *237*, 271.
(29) Scholes, D. S.; Ghiggino, K. P. *J. Phys. Chem*. **1994**, *98*, 8, 4580.
(30) Scholes, D. S.; Harcourt, D.; Ghiggino, K. P. *J. Chem. Phys*. **1995**, *102*, 9575.
(31) Claverie, P. In *Intermolecular Interactions: from Diatomics to Biopolymers*; Pullman, B. Ed.; Milley: New York, 1978.
(32) Scholes, D. G. In *Resonance Energy Transfer*; Andrews, D. L., Demidov, A. A., Eds.; Wiley: New York, 1998.
(33) Herzberg, G. In *Electronic Spectra and Electronic Sructure of Polyatomic Molecules*; Krieger, R. E., Ed.; Malabar Publishing Co.: Malabar, FL, 1991.
(34) Nakajima, A. *J. Lumin.* **1974**, *8*, 266.
(35) Strickler, S. J.; Berg, R. A. *J. Chem. Phys.* **1962**, *37*, 814.
(36) Chandrasekhar, S.; Ranganath, G. S. *Rep. Prog. Phys.* **1990**, *53*, 57. Munn, R. W. *Chem. Phys.* **1997**, *215*, 301.
(37) Birks, J. B. In *Organic Molecular Photophysics*; Birks, J. B. Ed.; John Wiley and Sons: New York, 1975. Vol. 2, p 494−502.
(38) Yakhot, V.; Cohen, M. D., Ludmer, Z. *Adv. Photochem.* **1979**, *11*, 489.
(39) Dong, R. Y.; Goldfarb, D. Moseley, M. E.; Luz, Z.; Zimmermann, H. *J. Chem. Phys.* **1984**, *88*, 3148.
(40) Nagamura, T.; Shigenobu, K. *J. Photochem. Photobiol. A* **1990**, *55*, 187.
(41) Evans, C. E.; Bohn, P. W. *J. Am. Chem. Soc*. **1993**, *115*, 3306.
(42) Nüesch, F.; Grätzel, M. *Chem. Phys.* **1995**, *193*, 50.
(43) Marguet, S.; Markovitsi, D. Manuscript in preparation.
(44) Levelut, A. M. *J. Phys. Lett.* **1986**, *124*, 478.
(45) Mun, R. W. *Chem. Phys.* **1997**, *215*, 301.
(46) Adam, D.; Schuhmacher, P.; Simmerer, J.; Häussling, L.; Siemens-meyer, K.; Etzbach, K. H.; Ringsdorf, H.; Haarer, D. *Nature* **1994**, *371*, 141.